



## Characterization of non-lipid autotaxin inhibitors

Adrienne B. Hoeglund<sup>a,b</sup>, Angela L. Howard<sup>a,b</sup>, Irene W. Wanjala<sup>a,b</sup>, Truc Chi T. Pham<sup>a</sup>, Abby L. Parrill<sup>a,b</sup>, Daniel L. Baker<sup>a,\*</sup>

<sup>a</sup> Department of Chemistry, The University of Memphis, Memphis, TN, United States

<sup>b</sup> Computational Research on Materials Institute, The University of Memphis, Memphis, TN, United States

### ARTICLE INFO

#### Article history:

Received 27 August 2009

Revised 23 November 2009

Accepted 24 November 2009

Available online 27 November 2009

#### Keywords:

Autotaxin, ATX

Nucleotide pyrophosphatase/

phosphodiesterase

FS-3

*para*-Nitrophenyl thymidine-5'-monophosphate

### ABSTRACT

Autotaxin (ATX) is a member of the ecto-nucleotide pyrophosphatase/phosphodiesterase (NPP) family and is a lysophospholipase D that cleaves the choline headgroup from lysophosphatidylcholine to generate the bioactive lipid lysophosphatidic acid (LPA). Enhanced expression of ATX and specific receptors for LPA in numerous cancer cell types has created an interest in studying ATX as a potential chemotherapeutic target. Likewise, ATX has been linked to several additional human diseases including multiple sclerosis, diabetes, obesity, neuropathic pain, and Alzheimer's disease. ATX inhibitors reported to date consist of metal ion chelators, lipid-like product analogs, and non-lipid small molecules. In the current research, we examined the pharmacology of the best of our previously reported non-lipid small molecule inhibitors. Here, these six inhibitors were studied utilizing the synthetic fluorescent lysophospholipid substrate FS-3, the nucleotide substrate pNP-TMP and the endogenous substrate LPC (16:0). All six compounds inhibited FS-3 hydrolysis  $\geq 50\%$ , whereas only three inhibited the hydrolysis of pNP-TMP to this degree. None of the six compounds blocked LPC 16:0 hydrolysis within the desired 50% inhibition range. The most potent analog (**5**, H2L 7905958) displayed an  $IC_{50}$  of 1.6  $\mu M$  ( $K_i = 1.9 \mu M$ , competitive inhibition) with respect to ATX-mediated FS-3 hydrolysis and an  $IC_{50}$  of 1.2  $\mu M$  ( $K_i = K'_i = 6.5 \mu M$ , non-competitive inhibition) against ATX-mediated pNP-TMP hydrolysis. All six inhibitors were specific for ATX as they were without affect on two additional lipid preferring NPP isoforms.

© 2009 Elsevier Ltd. All rights reserved.

### 1. Introduction

Autotaxin (ATX, NPP2) is a member of the ecto-nucleotide pyrophosphatase/phosphodiesterase (NPP) enzyme family. ATX was originally identified as a tumor cell autocrine motility factor from the conditioned medium of melanoma cells.<sup>1</sup> Since its discovery, increased ATX expression has been found in numerous human tumor cell lines including human teratocarcinoma,<sup>2</sup> hepatocellular carcinoma,<sup>3</sup> renal cell carcinoma,<sup>4</sup> metastatic breast cancer,<sup>5–7</sup> ovarian cancer,<sup>8</sup> neuroblastoma,<sup>9</sup> thyroid carcinoma,<sup>10</sup> prostate cancer,<sup>11</sup> follicular lymphoma,<sup>12</sup> Hodgkin lymphoma,<sup>13</sup> and invasive glioblastoma multiforme.<sup>14</sup> ATX has also been associated with several other human diseases including obesity,<sup>15–19</sup> neuropathic pain,<sup>20–22</sup> Alzheimer's disease,<sup>23</sup> arthritis,<sup>24,25</sup> and multiple sclerosis.<sup>26</sup>

The majority of biological effects elicited by ATX can be explained by its lysophospholipase D activity that hydrolyzes lysophosphatidylcholine (LPC) to produce lysophosphatidic acid (LPA) with subsequent activation of specific LPA receptors.<sup>27–31</sup> LPA is a lipid mediator with a wide variety of biological actions<sup>32,33</sup> including stimulation of cell proliferation,<sup>34,35</sup> cell migration,<sup>36</sup> tumor cell

invasion,<sup>37</sup> cell survival and angiogenesis.<sup>38</sup> LPA has been linked to the promotion and progression of cancer<sup>39</sup> and the production of LPA is consistent with the cancer-promoting actions of ATX.<sup>39</sup> Because of this, inhibition of ATX has become a desirable pharmacological target.

Since the first published ATX inhibitor (L-histidine) was reported,<sup>40</sup> two additional categories of inhibitors have been described. The first category, analogs of bioactive lipids including LPA,<sup>41–49</sup> lack significant structural diversity and lack characteristics<sup>50,51</sup> seen in the majority of orally bioavailable drugs. The second category consists of non-lipid small molecule inhibitors that exhibit increased structural diversity and have physiochemical characteristics more consistent with many oral drugs (see Figs. 1 and 2).<sup>52–54</sup>

Investigation of feedback effects performed by van Meeteren et al., demonstrated that LPA inhibited ATX-mediated hydrolysis of both LPC and synthetic non-lipid substrates.<sup>49</sup> While LPA is a potent and efficacious inhibitor of ATX activity, it cannot be a useful therapeutic agent as it promotes the pathologies that an ATX inhibitor would be directed to prevent.

The human NPP family contains seven isoforms (NPP1–7) numbered in the order of their identification as members of the family. Sequence identities and domain architecture indicate that ATX is

\* Corresponding author. Tel.: +1 901 678 4178; fax: +1 901 678 3447.

E-mail address: [dlbaker@memphis.edu](mailto:dlbaker@memphis.edu) (D.L. Baker).

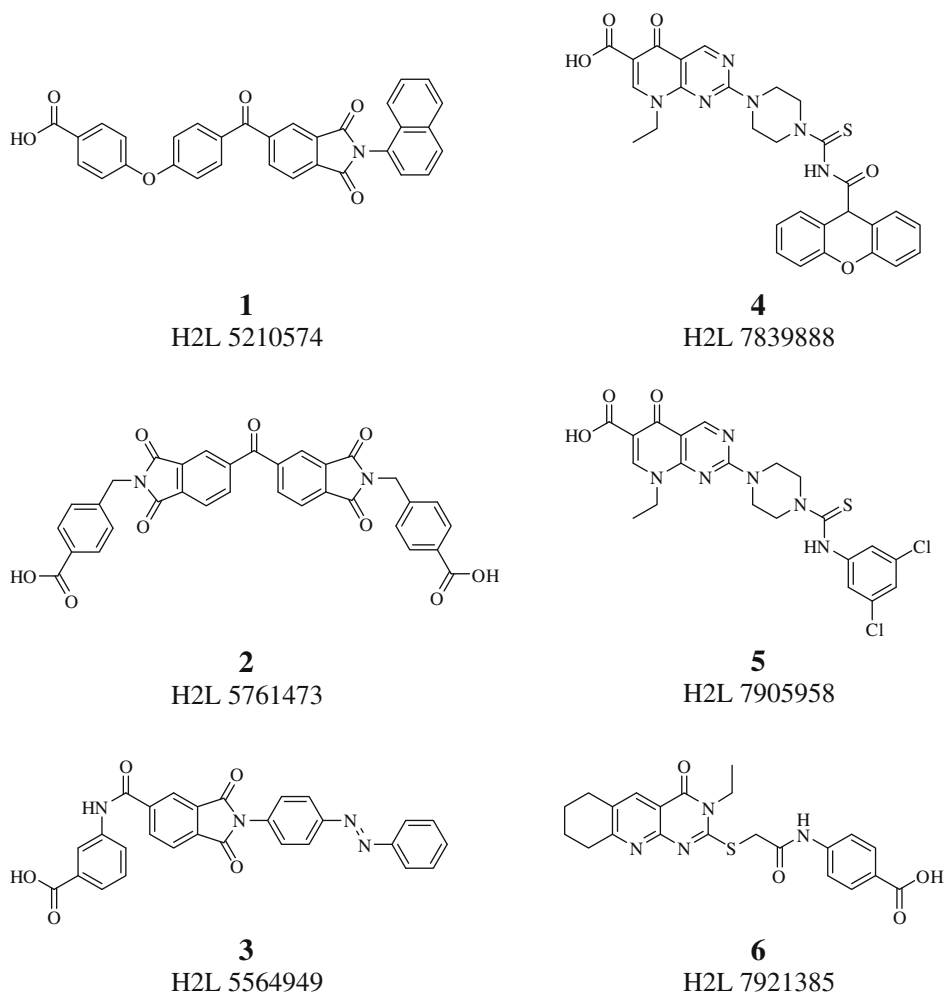


**Figure 1.** Structures of previously identified non-lipid ATX inhibitors obtained from ChemBridge.<sup>53</sup>

most similar to NPP1 and NPP3. However, ATX is most similar to NPP6 and NPP7 in terms of substrate recognition properties. NPP1 and NPP3 have been shown to preferentially hydrolyze nucleotide substrates,<sup>55–57</sup> whereas ATX, NPP6 and NPP7 have been shown to preferentially hydrolyze lipid substrates.<sup>55–57</sup> ATX, NPP6 and NPP7 all hydrolyze the lysophospholipid LPC although with differing regioselectivities. ATX cleaves LPC to form choline and LPA (lysophospholipase D activity) while NPP6 and NPP7 generate phosphocholine and monoacylglycerol as hydrolytic products (lysophospholipase C activity). The substrate specificities of NPP4 and NPP5 have yet to be described.

In this study, we characterized the pharmacology of the best of our previously published non-lipid small molecule ATX inhibitors, which had originally been studied only at single concentrations using FS-3 as substrate.<sup>53</sup> The potency of ATX inhibition for these compounds was studied here using three different substrates, one nucleotide analog (pNP-TMP) and two lipids (FS-3, and LPC 16:0). We found that three of the compounds inhibited the hydrolysis of both FS-3 and pNP-TMP by 50% or better at a single 10  $\mu$ M dose, while the remaining three inhibited only FS-3 hydrolysis at this level. These six compounds and LPA, all failed to inhibit >50% of ATX-mediated LPC 16:0 hydrolysis at the single dose using the Amplex<sup>®</sup> red based assay system. The  $K_i$  values for these compounds demonstrated low micromolar potency with FS-3 and pNP-TMP as substrate. The mechanism of ATX inhibition was determined for each compound to aid in the development of future QSAR models. Our long term goal is to develop models that will

predict both the probability of activity (i.e., ATX inhibition), the probable mechanism of that inhibition (competitive, uncompetitive, non-competitive, or mixed-mode), and affinity for the enzyme ( $K_i$ ). To further explore the pharmacology of these compounds, their selectivity for inhibition of the lysophospholipase D activity of ATX versus the lysophospholipase C activity of the NPP6 and NPP7 isoforms capable of LPC hydrolysis was examined.

## 2. Results

### 2.1. Potency determination

Previously, we used structure-based screening and binary QSAR approaches to prioritize a database of 868 compounds for experimental analysis as ATX inhibitors. Based on this prioritization, a total of 148 compounds were screened utilizing FS-3 hydrolysis by ATX as an endpoint. This analysis resulted in the identification of six leads that blocked ATX activity by  $\geq 50\%$  at a single inhibitor dose (10  $\mu$ M). Here we describe thorough characterization of these non-lipid, small molecule leads. First, inhibitors **1–6** were analyzed for auto fluorescence and for potential interference with the FS-3 fluorophore to exclude potential negative and positive interference, respectively. Compounds **1–6** lacked both significant auto fluorescence and effect on the fluorescence of carboxy-fluorescein, a model of the ATX generated FS-3 fluorophore (Fig. 3). Based on these results subsequent changes in measured fluorescence were deemed to be due to inhibition of ATX-mediated FS-3 hydrolysis

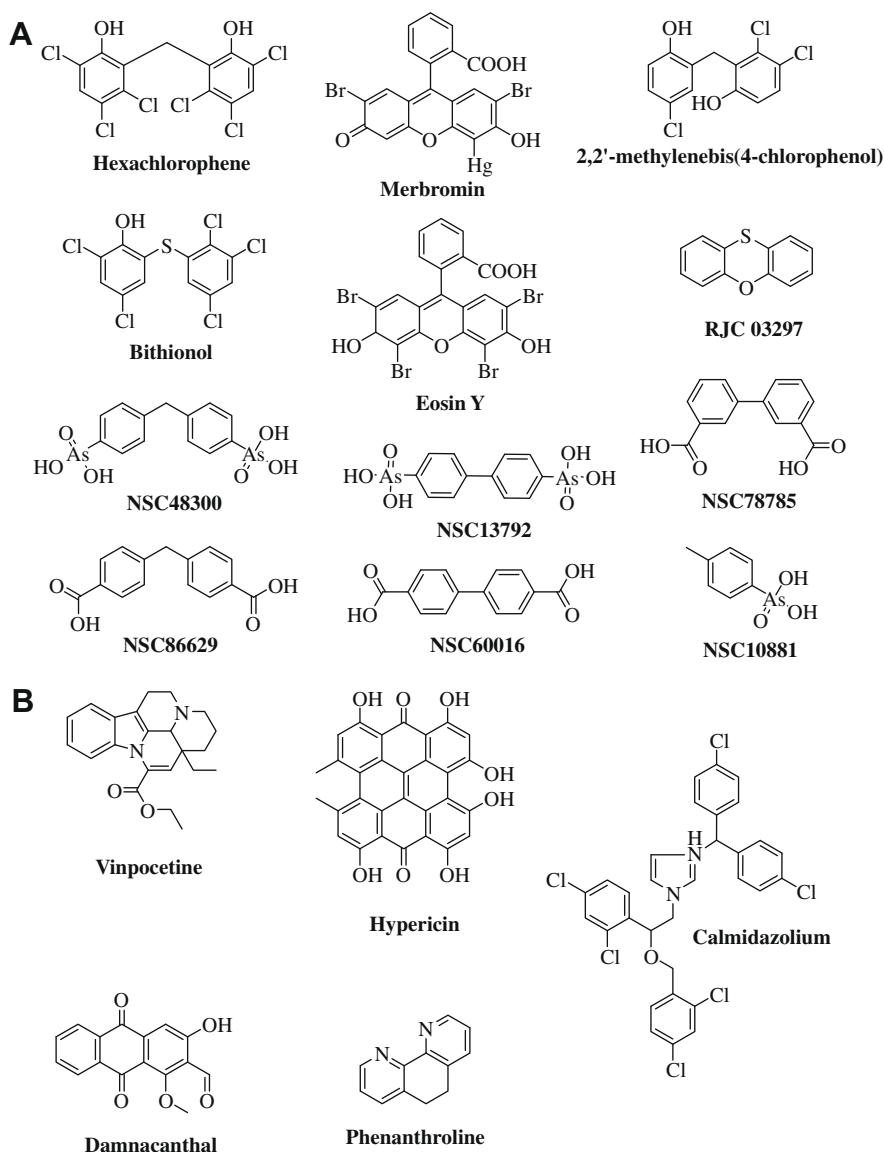


**Figure 2.** Structures of additional published non-lipid ATX inhibitors.<sup>52,54</sup> (A) Structures of NSC 48300 with its respective analogs. (B) Structures of PDE I inhibitors, Calmidazolium and Vinpocetine; kinase inhibitors Damnacanthal and Hypericine; and Phenanthroline.

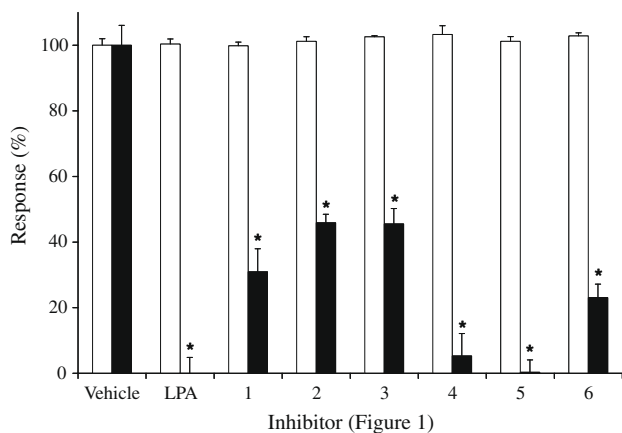


**Figure 3.** Inhibition of ATX-mediated FS-3 hydrolysis at a single dose (10  $\mu$ M). White bars represent compounds 1–6 in the presence of carboxy-fluorescein, black columns show the response to ATX-mediated hydrolysis of FS-3. None of the six compounds produced signal in the absence of carboxy-fluorescein alone. Statistically significant differences from vehicle control ( $p < 0.05$ ) are marked with \*.

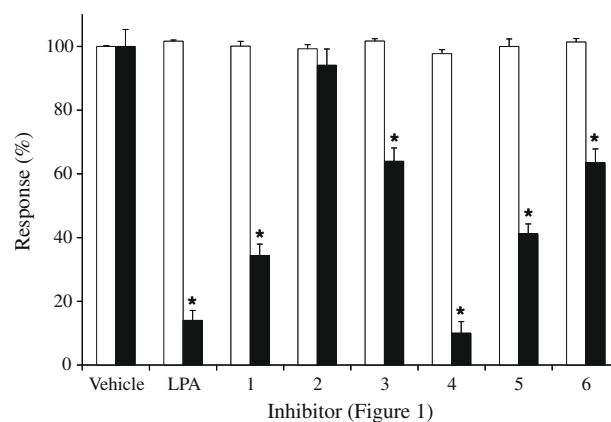


**Figure 4.** Inhibition of ATX-mediated pNP-TMP hydrolysis at a single dose (10  $\mu$ M). White bars represent compounds 1–6 in the presence of *p*-nitrophenol, black columns show the response to ATX-mediated hydrolysis of pNP-TMP. None of the six compounds produced signal in the absence of *p*-nitrophenol alone. Statistically significant differences from vehicle control ( $p < 0.05$ ) are marked with \*.

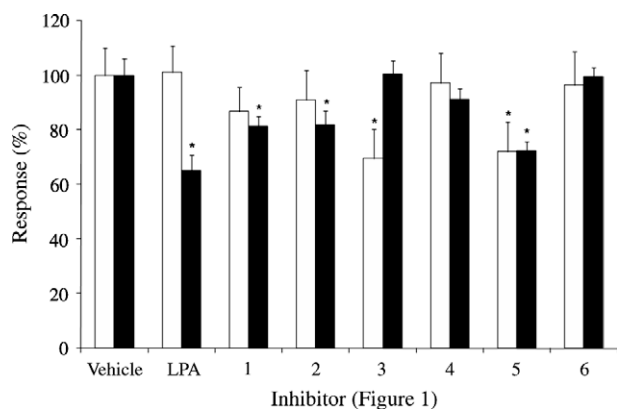


**Figure 5.** Inhibition of ATX-mediated LPC 16:0 hydrolysis at a single dose (10  $\mu$ M). White bars represent compounds **1–6** in the presence of choline and Amplex® red cocktail, black columns show the response to ATX-mediated hydrolysis of LPC. None of the six compounds produced signal in the absence of choline and Amplex® red cocktail. Statistically significant differences from vehicle control ( $p < 0.05$ ) are marked with \*.

alone. Compounds **1–6** and the positive control LPA 18:1 blocked ATX activity by  $\geq 50\%$  in this assay. Compound **5** shows efficacy similar to that of the positive control.

The six leads were also screened for inhibition of ATX using pNP-TMP and LPC (16:0) as ATX substrates. None of the six leads produced significant absorbance at 405 nm alone or significantly altered the absorbance of *p*-nitrophenol, the ATX generated product from pNP-TMP (Fig. 4). Compounds **1**, **4** and **5** (10  $\mu$ M) inhibited the hydrolysis of pNP-TMP within the 50% inhibition threshold, with compound **4** being as efficacious as the positive control (Fig. 4). Unlike the previously described assays, the presence of compounds **3** and **5** resulted in significant differences in the fluorescent signal generated by choline, the product of ATX hydrolysis of LPC. None of the six leads, nor the positive control LPA 18:1, inhibited ATX-mediated LPC hydrolysis by  $\geq 50\%$  as measured using the Amplex® red assay (Fig. 5).

The dose-response for ATX inhibition was determined for each compound using FS-3 and compounds **1**, **4** and **5** using pNP-TMP but not LPC as substrates (Fig. 6).  $IC_{50}$  values ranging from 1.5  $\mu$ M to 12.8  $\mu$ M were observed for ATX-mediated FS-3 hydrolysis and 1.2–6.8  $\mu$ M for pNP-TMP hydrolysis (Fig. 6). Compounds **4** and **5** were the most potent inhibitors of both FS-3 and pNP-TMP hydrolysis, exhibiting  $IC_{50}$  values of 1.5 and 1.6  $\mu$ M (FS-3) and 1.7 and 1.2  $\mu$ M (pNP-TMP), respectively. Despite complete inhibition of ATX-mediated hydrolysis of FS-3 by both **4** and **5** at high concentrations, only compound **4** was able to completely inhibit ATX-mediated hydrolysis of pNP-TMP at high concentrations.

### 2.1.1. Determination of inhibition kinetics and mechanism

The mechanism of enzyme inhibition was determined using simultaneous nonlinear regression of these kinetic data using equations for competitive, uncompetitive, mixed, and non-competitive kinetic inhibition. Kinetic data (initial rates) were determined for compounds **1–6** with FS-3 as substrate and for compounds **1**, **4**, and **5** with pNP-TMP as substrate. Representative data are shown for compound **5** in Figure 7. The mechanism yielding the lowest average percent residual error was selected in each case. The affinity for the enzyme,  $K_i$  (competitive, mixed, or non-competitive), and the affinity for the enzyme–substrate complex,  $K'_i$  (mixed, non-competitive, or uncompetitive), were determined during the simultaneous nonlinear regression analysis (Table 1). None of the inhibitors tested acted by uncompetitive inhibition, meaning each was capable of binding to the enzyme in the absence of substrate. Average  $K_m$  values of  $3.7 \pm 1.9 \mu$ M ( $n = 22$ ) for FS-3 and

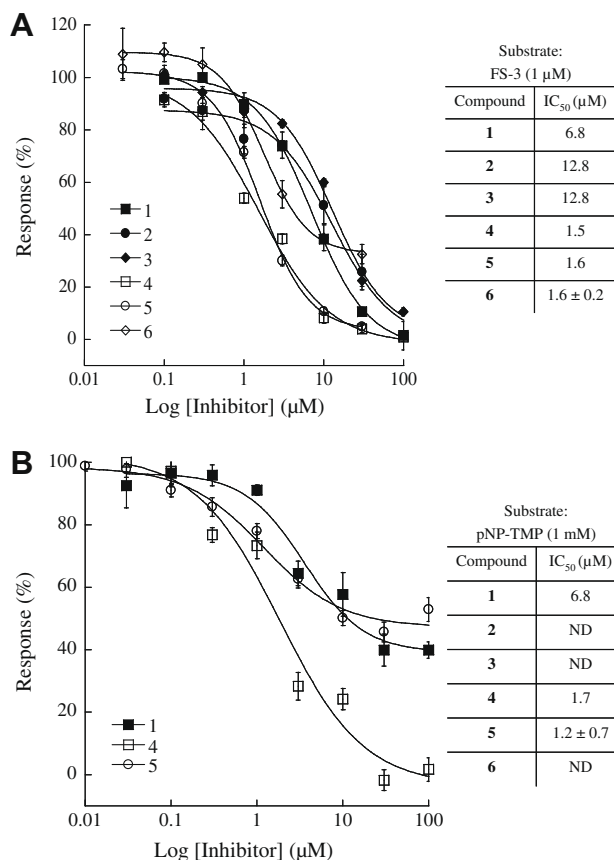


**Figure 6.** Dose-response curves for inhibition of ATX-mediated FS-3 (A) and pNP-TMP (B) hydrolysis. Errors shown are based on triplicate runs. ND indicates the dose response was not determined because these compounds did not hydrolyze pNP-TMP within the 50% inhibition threshold. If duplicate  $IC_{50}$  values were within  $\pm 3\%$ , determinations were based on two experiments and the values are shown as single numbers.

$5.6 \pm 1.3$  mM ( $n = 11$ ) for ATX-mediated pNP-TMP hydrolysis were determined from the zero inhibitor data. These data were used in all subsequent non-linear data analysis.

Compounds **1**, **3** and **4** showed mixed-mode inhibition against ATX-mediated FS-3 hydrolysis with  $K_i$  values ranging from 2.7 to 15.1  $\mu$ M. These compounds showed significantly higher  $K'_i$  values (19.8–40.3  $\mu$ M) which denotes reduced affinity for the enzyme–substrate complex over that of free enzyme. Compounds **2** and **5** were competitive ATX inhibitors with  $K_i$  values ranging from 1.9 (**5**) to 5.0 (**2**)  $\mu$ M. Compound **6** showed non-competitive inhibition with  $K_i = K'_i = 9.3 \mu$ M.

Interestingly, the mechanism of inhibition for ATX-mediated hydrolysis of the nucleotide analog pNP-TMP was not always the same as that for ATX-mediated FS-3 hydrolysis. Compound **4** showed competitive inhibition for pNP-TMP hydrolysis with a  $K_i$  of 2.7  $\mu$ M in contrast to the mixed-mode inhibition observed with FS-3. Likewise, compound **5** showed non-competitive inhibition with a  $K_i = K'_i = 6.5 \mu$ M in contrast to the competitive inhibition observed with FS-3. The mechanism of inhibition for compounds **2**, **3**, and **6** was not determined for ATX-mediated pNP-TMP hydrolysis due to their low efficacies at single 10  $\mu$ M doses in the presence of this substrate. Mechanism of inhibition was not determined for any of the compounds with respect to ATX-mediated LPC 16:0 hydrolysis.

### 2.1.2. NPP isoform selectivity

We also examined the selectivity of compounds **1–6** by examining their effects against NPP6 and NPP7, the only other currently

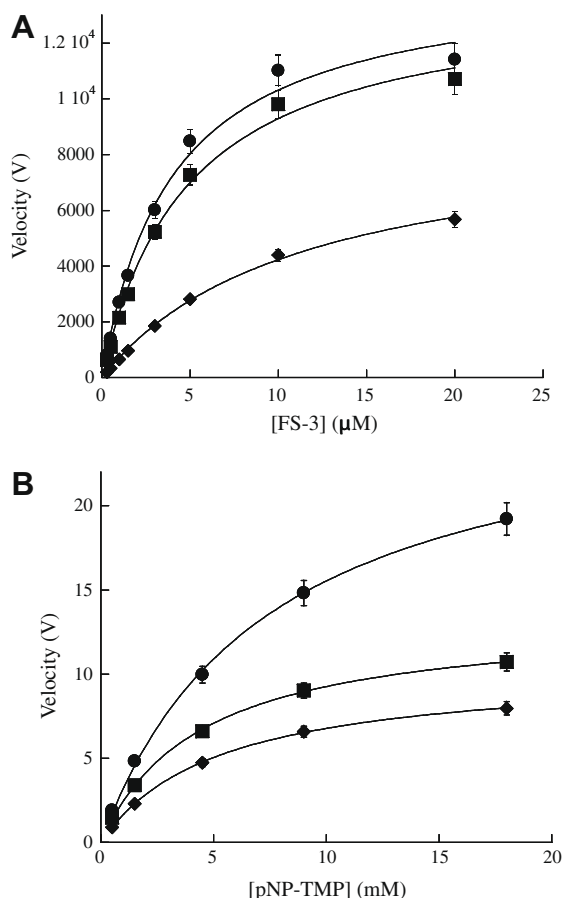


**Figure 7.** Inhibition of ATX activity by compound 5. (A) Inhibitor concentrations from top to bottom 0, 1 and 10 μM on the plate. (B) Inhibitor concentrations from top to bottom 0, 1 and 10 μM on the plate.

known lipid preferring NPP isoforms. Inhibition of the hydrolysis of *p*-nitrophenylphosphorylcholine by NPP6 and NPP7 was determined via the production of *p*-nitrophenol by measuring absorbance at 405 nm. None of these six compounds inhibited the

**Table 1**  
Inhibitor  $K_i$  and  $K_i'$  values for ATX-mediated FS-3 and pNP-TMP hydrolysis

Inhibitor ID ([low],[high])	FS-3		
	Inhibition mechanism	$K_i$ (μM)	$K_i'$ (μM)
1 (4, 12)	Mixed	5.8	32.3
2 (6, 12)	Competitive	5.0	—
3 (12, 24)	Mixed	15.1	40.3
4 (6, 12)	Mixed	2.7	19.8
5 (1, 10)	Competitive	1.9	—
6 (3, 10)	Non-competitive	9.3	9.3
<i>pNP-TMP</i>			
1	ND	—	—
2	ND	—	—
3	ND	—	—
4 (0.87, 3.48)	Competitive	2.7	—
5 (1, 10)	Non-competitive	6.5	6.5
6	ND	—	—

Values next to the compound identification number identify the low ( $\sim 0.5 \times IC_{50}$ ) and high ( $\sim 2 \times IC_{50}$ ) inhibitor concentrations (μM) used for each compound. The averaged percent residual errors for the FS-3 and pNP-TMP mechanism of inhibition determinations were consistently less than 10% or in the range of 10–17%, respectively.

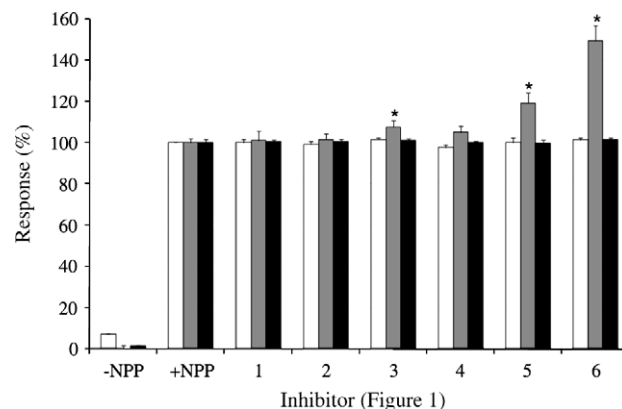


**Figure 8.** Effect of leads 1–6 on NPP6 and NPP7 activity at single doses (10 μM). White bars represent compounds 1–6 in the presence of *p*-nitrophenol, grey represents effect on the NPP6 isoform, and black bars represent effect on the NPP7 isoform. Statistically significant differences from vehicle control ( $p < 0.05$ ) are marked with \*.

activity of NPP6 or NPP7 (Fig. 8). As a matter of interest, compound 6 slightly increased the response of NPP6. The reason for this effect requires further analysis.

### 3. Discussion

Interest in ATX as a therapeutic target has grown significantly since the identification of its recently described lysoPLD activity.<sup>27,28</sup> This interest has resulted in the identification of three distinct categories of ATX inhibitors, metal chelators, and small molecules that are either lipid-like or non-lipids. In the current study, we report the further characterization of the potency, mechanism of inhibition and enzymatic selectivity of six previously identified non-lipid, small molecule inhibitors of ATX.

The first reported ATX inhibitors were compounds known to chelate metal ions.<sup>40,58</sup> L-Histidine, EDTA, and 1,10-phenanthroline have been shown to inhibit ATX activity in the millimolar concentration range.<sup>40,58</sup> These inhibitors are thought to compete with active site histidine and aspartic acid residues for divalent metal ions.<sup>40</sup> However, inhibition of ATX via metal ion chelation is both relatively insensitive and likely to be nonspecific. van Meeteren et al. were the first to report the feed back inhibition of ATX by the bioactive lipids LPA and S1P.<sup>49</sup> This discovery led to the characterization of several lipid analogs (with nanomolar to micromolar potencies) as ATX inhibitors.<sup>29,41,42,44–49,59,60</sup> While these analogs have shown promise in *in vitro* assays, they do not meet many of the rules described by Lipinski for orally bioavailable drugs.<sup>50,51</sup> Therefore, questions remain concerning their pharmacokinetics and pharmacodynamics and thus the utility of these reagents as future therapeutics.

Non-lipid small molecule inhibitors of ATX have also been described. In contrast to lipid-like compounds, the described non-lipid ATX inhibitors possess more of the characteristics of orally bioavailable drugs. Recently, Saunders et al. used high throughput screening to identify an ATX inhibitor with nanomolar potency (NSC38200).<sup>54</sup> Likewise, Moulharat et al. used a library of known kinase inhibitors, including the previously identified p56lck tyrosine kinase inhibitor, damnacanthal, to identify ATX inhibitors with potencies in the millimolar range.<sup>52,54</sup> Finally, our group used a binary QSAR, virtual screening approach to examine over 800 small molecules that resulted in the identification of six efficacious ATX inhibitors.<sup>53</sup> These six leads (Fig. 1) exhibit low micromolar potencies against ATX-mediated FS-3 and pNP-TMP hydrolysis (Table 1) which is comparable to previously published ATX inhibitors.<sup>29,41,42,44–49,59,60</sup>



Here we have used three different substrates to evaluate potential ATX inhibitors including the endogenous substrate LPC (16:0). Previous work utilized LPC in the characterization of ATX inhibitors.<sup>40,42,44,46,49,52,59</sup> However, LPC may not be as straightforward as other substrates in the characterization of small molecule ATX inhibitors. Moulharat and colleagues reported that while the kinase inhibitor damnacanthol exhibited micromolar potency using pNPPP (*para*-nitrophenyl phenylphosphate) as a substrate ( $IC_{50} = 17 \pm 6.3 \mu M$ ,  $n = 2$ ), its  $IC_{50}$  increased approximately eight-fold ( $IC_{50} = 139 \pm 21 \mu M$ ,  $n = 3$ ) when LPC was used as substrate.<sup>52</sup> However,  $IC_{50}$  values are influenced by both the substrate  $K_m$  and substrate concentration, thus these values should not be compared directly.  $K_i$  values representing inhibitor affinity for the enzyme were not reported. Here, we assayed compounds **1–6** using an Amplex<sup>®</sup> red based assay with LPC 16:0 as substrate (Fig. 5). In all cases, significantly less inhibition of ATX-mediated hydrolysis of LPC at a single 10  $\mu M$  dose was noted than for ATX-mediated hydrolysis of FS-3 or pNP-TMP. Further investigation showed that compounds **1–6** resulted in varying degrees of interference in the presence of choline (as a positive control). Additionally, LPA failed to show substantial inhibition in the Amplex<sup>®</sup> red assay although it has previously been demonstrated to inhibit hydrolysis of radiolabeled LPC in a simpler, but low-throughput assay system.<sup>49</sup> Thus, our future work involving the identification of ATX inhibitors will exclude the LPC/Amplex<sup>®</sup> red assay as a primary screening tool.

ATX, NPP6 and NPP7 are the only known NPP isoforms that prefer lipid substrates.<sup>55–57</sup> Despite differences in regioselectivity (lysophospholipase D for ATX versus lysophospholipase C activity for NPP6/7), the ability for all three isoforms to utilize LPC as substrate suggests potential overlap in inhibitor recognition/sensitivity. To our knowledge this is the first known report where the NPP selectivity of ATX inhibitors has been evaluated. The six compounds characterized herein are ATX specific in that they failed to inhibit NPP6 and NPP7. Further characterization will need to be conducted to ensure a lack of other off-target effects.

To date, few publications have described the kinetics of ATX inhibition. L-Histidine inhibition of ATX activity was reported to be non-competitive based on a reduction in  $V_{max}$  with no apparent change in  $K_m$ .<sup>40</sup> LPA was characterized as a mixed-mode ATX inhibitor via effects on both  $K_m$  and  $V_{max}$ , implying interaction with both enzyme and enzyme–substrate complexes.<sup>49</sup> FTY720-phosphate and S32826 were identified as competitive ATX inhibitors through an increase in the apparent  $K_m$ .<sup>46,61</sup> As of the writing of this paper, only Saunders et al. had reported on the kinetics of ATX inhibition by non-lipids.<sup>54</sup> In their work NSC 48300 was identified as a competitive inhibitor due to an increase in  $K_m$  and no change in  $V_{max}$ .<sup>54</sup> Although structural similarities exist between compounds **1–6**, three modes of inhibition were observed in our analysis. Mixed-mode inhibition of ATX-mediated FS-3 hydrolysis was noted for compounds **1**, **3**, and **4**, whereas compound **2** exhibited competitive inhibition and compound **6** was a non-competitive inhibitor. Inhibitors acting by these three mechanisms share the ability to bind to the free enzyme (characterized by  $K_i$ ), a property that is independent of substrate identity. The identical  $K_i$  values obtained for compound **4** using both FS-3 and pNP-TMP as substrate (2.7  $\mu M$ ) reflect this substrate independence. The range of  $K_i$  values for compound **5** with the two substrates (1.9–6.5  $\mu M$ ) suggest the precision of  $K_i$  determination. Assays with FS-3 are more reproducible in our hands, and give lower fitting errors, thus we regard the former value as more representative of the true  $K_i$  for compound **5**. Mixed and non-competitive inhibitors have the additional ability to bind to the enzyme–substrate complex (characterized by  $K'_i$ ), a property that is clearly dependent on substrate identity. The inhibition mechanism differences observed, for example, when compound **4** was tested with FS-3 (mixed) and pNP-TMP (competitive), reflect the substrate-dependence of binding to the

enzyme–substrate complex. These results suggest that compounds **1–6** will be effective in assays that will reflect the inhibition of the hydrolysis of LPC without the complications presented by the Amplex<sup>®</sup> red system.

## 4. Conclusions

Here six previously identified, non-lipid small molecule ATX inhibitors were characterized at single concentrations using lipid and nucleotide substrate analogs, by dose response determinations, mechanism of inhibition examinations and for selectivity against other lipid-preferring NPP isoforms.  $IC_{50}$  values from 1.2 to 12.8  $\mu M$  were identified. Compounds **1**, **3** and **4** exhibited mixed-mode inhibition against FS-3 with  $K_i$  values ranging from 2.7 to 15.1  $\mu M$ . Compound **2**, with a  $K_i$  of 5.0  $\mu M$ , compound **5** with a  $K_i$  of 1.9  $\mu M$  and compound **4** with a  $K_i$  of 2.7  $\mu M$ , exhibited competitive inhibition against FS-3 (**2,5**) and pNP-TMP (**4**), respectively. Compound **6** ( $K_i = 9.3 \mu M$ ) and compound **5** ( $K_i = 6.5 \mu M$ ) showed non-competitive inhibition against FS-3 (**6**) and pNP-TMP (**5**). Compounds **1–6** were shown to be specific for ATX over the NPP6 and NPP7 isoforms. Notably, all inhibitors shared the ability to bind to free ATX, suggesting that the inhibition has potential transferability to cellular and in vivo assays. Further studies are underway in an attempt to derive further structure activity relationship data for ATX inhibition from these leads.

## 5. Materials and methods

### 5.1. ATX inhibition assays

ATX inhibition was assayed using the synthetic FRET-based lysophospholipid analog FS-3 (Echelon Biosciences, Inc., Salt Lake City, UT), a synthetic nucleotide analog *para*-nitrophenyl thymidine-5'-monophosphate (pNP-TMP) (Sigma Aldrich, St. Louis, MO), and the presumed endogenous substrate LPC 16:0 (Avanti Polar Lipids, Alabaster, AL). The inhibitors, H2L 5210574 (**1**), H2L 5761473 (**2**), H2L 5564949 (**3**), H2L 7839888 (**4**), H2L 7905958 (**5**), and H2L 7921385 (**6**), were obtained from ChemBridge Corporation (San Diego, CA). All three assays used ~10 times concentrated conditioned medium (CCM) from MDA-MB-435 cells as the source of ATX. The FS-3 and pNP-TMP assays used CCM without further manipulation, whereas the LPC (16:0) assay, based on the Amplex<sup>®</sup> red protocol,<sup>62</sup> utilized CCM that was exchanged into assay buffer (50 mM Tris pH 7.4, 5 mM  $CaCl_2$  and 1 mg/mL BSA) using a 30 kDa molecular weight cutoff filter in an Amicon pressure cell (Millipore, Beverly, MA). Studies with other inhibitors not reported here have demonstrated that recombinant purified ATX and that obtained from CCM give the same rank order of efficacy and absolute efficacies were within 10% using the two enzyme sources (data not shown).

MDA-MB-435 cells were cultured at 37 °C under a humidified atmosphere containing 5%  $CO_2$  in Dulbecco's Modified Eagle Medium (DMEM) (MediaTech, Herndon, VA) containing 100 U/ml penicillin, 100  $\mu g$ /ml streptomycin (Hyclone, Logan, UT), 5% fetal bovine serum (FBS) (Hyclone, Logan, UT), and 2 mM L-glutamine (Hyclone, Logan, UT). Cells were grown to ~80% confluence, at which time the cells were washed twice with sterile phosphate buffered saline prior to the addition of serum free DMEM containing L-glutamine and antibiotics. Conditioned medium was collected after 48 h and supplemented with 10% ethylene glycol. The media was concentrated ~10-fold and buffer exchanged into Tris (50 mM, pH 7.4) containing 20% ethylene glycol using an Amicon 8050 cell (Millipore, Beverly, MA) fitted with a PM30 filter (Millipore, Billerica, MA). Aliquots of 10 $\times$  conditioned media (source of ATX) were stored at 4 °C.

All assays were performed in 96-well half-area plates (Corning Inc, Lowell, MA) at 37 °C with data read at 2 min intervals using a Synergy2 system (BioTek, Winooski, VT). For determination of effect on ATX-mediated hydrolysis of FS-3 assay wells (60 µL) contained CCM (20 µL) and inhibitor (10 µM) with FS-3 (1 µM) and charcoal-stripped<sup>63</sup> fatty acid free BSA (30 µM) in assay buffer (1 mM each CaCl<sub>2</sub> and MgCl<sub>2</sub>, 5 mM KCl, 140 mM NaCl, 50 mM Tris pH 8.0). Fluorescence was monitored with excitation at 485 nm and emission at 528 nm.<sup>64</sup> To monitor ATX-mediated hydrolysis of pNP-TMP, substrate was maintained at 1 mM and absorbance was measured at 405 nm.<sup>49</sup> For analysis of affect on ATX-mediated hydrolysis of LPC 16:0, substrate consisted of 150 µM LPC (16:0). An additional Amplex<sup>®</sup> red cocktail (comprised of 10 µM Amplex<sup>®</sup> red, 0.3 mM choline oxidase and 3 µM horseradish peroxidase) was also included. The production of resorufin was monitored by fluorimetry using excitation at 530 nm and emission at 590 nm.<sup>62,65</sup> All experiments were repeated at least twice and typical results are shown. The student's *t* test was used to determine statistically significant differences from vehicle control using GraphPad. Any comparison with *p* < 0.05 was identified as being statistically significant.

## 5.2. Assay interference

To confirm that the inhibitors did not provide false positive or false negative results by quenching or enhancing the fluorescent or absorbance signals, control experiments were run. For ATX-mediated FS-3 hydrolysis, carboxy-fluorescein (Sigma-Aldrich, St. Louis, MO) was used as an analog of the FS-3 hydrolytic product fluorophore. Assay wells (60 µL) contained each lead compound (10 µM) with charcoal stripped BSA<sup>63</sup> (30 µM) in assay buffer as described, in the absence or presence of carboxy-fluorescein (200 nM). All assays were performed in 96-well plates with data read at a single point using a Synergy2 system (BioTek, Winooski, VT). Fluorescence was monitored using excitation at 485 nm and emission at 528 nm. For ATX-mediated pNP-TMP hydrolysis, leads were assayed in the absence and presence of *p*-nitrophenol (10 µM) and absorbance at 405 nm was determined. For ATX-mediated LPC 16:0 hydrolysis, inhibitors were analyzed in the absence and presence of choline (1 µM) and Amplex<sup>®</sup> red cocktail with fluorescence using 530 nm (excitation) and 590 nm (emission).

## 5.3. Kinetics analysis of ATX inhibition

Inhibition kinetics were determined using eight different concentrations of substrate (FS-3 and pNP-TMP) and three different concentrations (0, ~0.5 and ~2 times the IC<sub>50</sub>) of each inhibitor. The final FS-3 concentrations ranged from 0.3 to 20 µM, while the final pNP-TMP concentrations ranged from 0.25 to 33.33 mM. Normalized fluorescence or absorbance results were plotted as a function of time to determine initial rates. Initial rates for zero inhibitor concentrations were then plotted against substrate concentration and a rectangular hyperbolic curve was fitted using KaleidaGraph (version 4.03, Synergy Software, Reading, PA) to calculate *K<sub>m</sub>*. Data for all three inhibitor concentrations were simultaneously fitted in the Michealis–Menton equations for competitive, uncompetitive, mixed-mode, and non-competitive inhibition (shown below) using simultaneous non-linear regression for each model using WinNonLin<sup>®</sup> 6.1 (Pharsight, Mountain View, CA). Mechanism of inhibition was assigned to the model giving the lowest average percent residuals. *K<sub>i</sub>* and *K'<sub>i</sub>* values represent compound affinity for free enzyme and the enzyme–substrate complex, respectively.

- For competitive inhibition:  $V_o = \frac{V_{max}[S]}{\alpha K_m + [S]}$ , where  $\alpha = 1 + \frac{[I]}{K_i}$
- For mixed-mode inhibition:  $V_o = \frac{V_{max}[S]}{\alpha K_m + \alpha' [S]}$ , where  $\alpha' = 1 + \frac{[I]}{K'_i}$

- For non-competitive inhibition: ( $\alpha = \alpha'$ ), therefore:  $V_o = \frac{V_{max}[S]}{\alpha(K_m + [S])}$
- For uncompetitive inhibition:  $V_o = \frac{V_{max}[S]}{K_m + \alpha' [S]}$

## 5.4. NPP6 and NPP7 selectivity

ATX inhibitor selectivity was assayed using *p*-nitrophenylphosphorylcholine (pNPPC) (Sigma Aldrich, St. Louis, MO) as substrate for NPP6 and NPP7, the only other known lipid preferring NPP isoforms.<sup>57</sup> Assays were performed with conditioned media (CM or CCM) from HEK293 cells transiently transfected with NPP6 or NPP7. HEK293 cells were plated in Dulbecco's modified Eagle's medium (DMEM) (MediaTech, Herndon, VA) containing 10% fetal bovine serum, 100 U/ml penicillin, 100 µg/ml streptomycin (Hyclone, Logan, UT), and 2 mM L-glutamine. Cells were grown overnight at 37 °C under 5% CO<sub>2</sub> to ~80% confluence. Cells were then transfected with soluble constructs of NPP6<sup>56</sup> and NPP7<sup>66</sup> in the pCDNA3.1(+) mammalian expression vector using the Polyfect transfection reagent (Hyclone, Logan, UT) according to the manufacturer's protocol. Six hours after transfection, the medium was exchanged for serum free DMEM containing L-glutamine and antibiotics and the cells were incubated for an additional 48 h. Expressed protein was collected and concentrated (for NPP7) using 10 kDa molecular weight cutoff filters (Millipore, Beverly, MA). The final pNPPC concentration was 10 µM for NPP6 and 1 µM for NPP7. Assays were performed in 96-well plates with CM (NPP6) and CCM (NPP7) comprised of one-third of the total volume. The final volume was comprised of the substrate (pNPPC) in assay buffer and 10 µM inhibitor. Assay buffers for NPP6 (500 mM NaCl, 0.05% Triton X-100, 100 mM Tris-HCl (pH 9.0))<sup>56</sup> and NPP7 (50 mM tris HCl, pH 8.5, 150 mM NaCl, and 10 mM taurocholic acid)<sup>66–68</sup> were based on prior reports. However, unlike the published methods,<sup>66–68</sup> EDTA was not added to the NPP7 assay buffer. Absorbance was read at 2 minute intervals using a Synergy2 system (BioTek, Winooski, VT) at 405 nm. Results are shown at the 1 h time point, where all absorbance changes as a function of time were linear. Readings were normalized to vehicle control after subtraction of absorbance in the absence of CM/CCM. Data are shown as the mean ± SD of at least three wells. All experiments were repeated twice and representative results are shown. The student's *t* test was used to determine statistically significant differences from the vehicle control using GraphPad. Any comparison with *p* < 0.05 was identified as being statistically significant.

## Acknowledgement

This work was supported, in part, by a research grant from the Elsa U. Pardee Foundation (ALP and DLB).

## References and notes

- Stracke, M. L.; Arestad, A.; Levine, M.; Krutzsch, H. C.; Liotta, L. A. *Melanoma Res.* **1995**, *5*, 203.
- Lee, H. Y.; Murata, J.; Clair, T.; Polymeropoulos, M. H.; Torres, R.; Manrow, R. E.; Liotta, L. A.; Stracke, M. L. *Biochem. Biophys. Res. Commun.* **1996**, *218*, 714.
- Zhang, G.; Zhao, Z.; Xu, S.; Ni, L.; Wang, X. *Chin. Med. J. (Engl)* **1999**, *112*, 330.
- Stassar, M. J.; Devitt, G.; Brosius, M.; Rinnab, L.; Prang, J.; Schradin, T.; Simon, J.; Petersen, S.; Kopp-Schneider, A.; Zoller, M. *Br. J. Cancer* **2001**, *85*, 1372.
- Euer, N.; Schwirzke, M.; Evtimova, V.; Burtcher, H.; Jarsch, M.; Tarin, D.; Weidle, U. H. *Anticancer Res.* **2002**, *22*, 733.
- Chen, M.; O'Connor, K. L. *Oncogene* **2005**, *24*, 5125.
- Song, J.; Clair, T.; Noh, J. H.; Eun, J. W.; Ryu, S. Y.; Lee, S. N.; Ahn, Y. M.; Kim, S. Y.; Lee, S. H.; Park, W. S.; Yoo, N. J.; Lee, J. Y.; Nam, S. W. *Biochem. Biophys. Res. Commun.* **2005**, *337*, 967.
- Ptaszynska, M. M.; Pendrak, M. L.; Bandle, R. W.; Stracke, M. L.; Roberts, D. D. *Mol. Cancer Res.* **2008**, *6*, 352.
- Kawagoe, H.; Stracke, M. L.; Nakamura, H.; Sano, K. *Cancer Res.* **1997**, *57*, 2516.
- Kehlen, A.; Englert, N.; Seifert, A.; Klonisch, T.; Dralle, H.; Langner, J.; Hoang-Vu, C. *Int. J. Cancer* **2004**, *109*, 833.
- Zeng, Y.; Kakehi, Y.; Noh, M. A.; Tsunemori, H.; Sugimoto, M.; Wu, X. X. *Prostate* **2009**, *69*, 283.

12. Masuda, A.; Nakamura, K.; Izutsu, K.; Igarashi, K.; Ohkawa, R.; Jona, M.; Higashi, K.; Yokota, H.; Okudaira, S.; Kishimoto, T.; Watanabe, T.; Koike, Y.; Ikeda, H.; Kozai, Y.; Kurokawa, M.; Aoki, J.; Yatomi, Y. *Br. J. Haematol.* **2008**, *143*, 60.
13. Baumforth, K. R.; Flavell, J. R.; Reynolds, G. M.; Davies, G.; Pettit, T. R.; Wei, W.; Morgan, S.; Stankovic, T.; Kishi, Y.; Arai, H.; Nowakova, M.; Pratt, G.; Aoki, J.; Wakelam, M. J.; Young, L. S.; Murray, P. G. *Blood* **2005**, *106*, 2138.
14. Hoelzinger, D. B.; Mariani, L.; Weis, J.; Woyke, T.; Berens, T. J.; McDonough, W. S.; Sloan, A.; Coons, S. W.; Berens, M. E. *Neoplasia* **2005**, *7*, 7.
15. Ferry, G.; Tellier, E.; Try, A.; Grés, S.; Naime, I.; Simon, M. F.; Rodriguez, M.; Boucher, J.; Tack, I.; Gesta, S.; Chomarat, P.; Dieu, M.; Raes, M.; Galizzi, J. P.; Valet, P.; Boutin, J. A.; Saulnier-Blache, J. S. *J. Biol. Chem.* **2003**, *278*, 18162.
16. Boucher, J.; Quilliot, D.; Praderes, J. P.; Simon, M. F.; Gres, S.; Guigne, C.; Prevot, D.; Ferry, G.; Boutin, J. A.; Carpenne, C.; Valet, P.; Saulnier-Blache, J. S. *Diabetologia* **2005**, *48*, 569.
17. Gesta, S.; Simon, M. F.; Rey, A.; Sibrac, D.; Girard, A.; Lafontan, M.; Valet, P.; Saulnier-Blache, J. S. *J. Lipid Res.* **2002**, *43*, 904.
18. Simon, M. F.; Daviaud, D.; Pradere, J. P.; Gres, S.; Guigne, C.; Wabitsch, M.; Chun, J.; Valet, P.; Saulnier-Blache, J. S. *J. Biol. Chem.* **2005**, *280*, 14656.
19. Simon, M. F.; Rey, A.; Castan-Laurel, I.; Gres, S.; Sibrac, D.; Valet, P.; Saulnier-Blache, J. S. *J. Biol. Chem.* **2002**, *277*, 23131.
20. Inoue, M.; Ma, L.; Aoki, J.; Chun, J.; Ueda, H. *Mol. Pain* **2008**, *4*, 6.
21. Inoue, M.; Xie, W.; Matsushita, Y.; Chun, J.; Aoki, J.; Ueda, H. *Neuroscience* **2008**, *152*, 296.
22. Inoue, M.; Ma, L.; Aoki, J.; Ueda, H. *J. Neurochem.* **2008**, *107*, 1556.
23. Umemura, K.; Yamashita, N.; Yu, X.; Arima, K.; Asada, T.; Makifuchi, T.; Murayama, S.; Saito, Y.; Kanamaru, K.; Goto, Y.; Kohsaka, S.; Kanazawa, I.; Kimura, H. *Neurosci. Lett.* **2006**, *400*, 97.
24. Kehlen, A.; Lauterbach, R.; Santos, A. N.; Thiele, K.; Kabisch, U.; Weber, E.; Riemann, D.; Langner, J. *Clin. Exp. Immunol.* **2001**, *123*, 147.
25. Santos, A. N.; Riemann, D.; Santos, A. N.; Kehlen, A.; Thiele, K.; Langner, J. *Biochem. Biophys. Res. Commun.* **1996**, *229*, 419.
26. Hammack, B. N.; Fung, K. Y.; Hunsucker, S. W.; Duncan, M. W.; Burgoon, M. P.; Owens, G. P.; Gilden, D. H. *Mult. Scler.* **2004**, *10*, 245.
27. Tokumura, A.; Majima, E.; Kariya, Y.; Tominaga, K.; Kogure, K.; Yasuda, K.; Fukuzawa, K. *J. Biol. Chem.* **2002**, *277*, 39436.
28. Umezu-Goto, M.; Kishi, Y.; Taira, A.; Hama, K.; Dohmae, N.; Takio, K.; Yamori, T.; Mills, G. B.; Inoue, K.; Aoki, J.; Arai, H. *J. Cell Biol.* **2002**, *158*, 227.
29. Federico, L.; Pamuklar, Z.; Smyth, S. S.; Morris, A. J. *Curr. Drug Targets* **2008**, *9*, 698.
30. Moolenaar, W. H. *J. Cell Biol.* **2002**, *158*, 197.
31. Xie, Y.; Meier, K. E. *Cell. Signal.* **2004**, *16*, 975.
32. Tigyi, G.; Parrill, A. L. *Prog. Lipid Res.* **2003**, *42*, 498.
33. Moolenaar, W. H. *Trends Cell Biol.* **1994**, *4*, 213.
34. Contos, J. J.; Ishii, I.; Chun, J. *Mol. Pharmacol.* **2000**, *58*, 1188.
35. Moolenaar, W. H. *Exp. Cell Res.* **1999**, *253*, 230.
36. Kohn, E. C.; Hollister, G. H.; DiPersio, J. D.; Wahl, S.; Liotta, L. A.; Schiffmann, E. *Int. J. Cancer* **1993**, *53*, 968.
37. Nam, S. W.; Clair, T.; Campo, C. K.; Lee, H. Y.; Liotta, L. A.; Stracke, M. L. *Oncogene* **2000**, *19*, 241.
38. Nam, S. W.; Clair, T.; Kam, Y.-S.; McMarlin, A.; Schiffmann, E.; Liotta, L. A.; Stracke, M. L. *Cancer Res.* **2001**, *61*, 6938.
39. Mills, G. B.; Moolenaar, W. H. *Nat. Rev. Cancer* **2003**, *3*, 582.
40. Clair, T.; Koh, E.; Ptaszynska, M.; Bandle, R. W.; Liotta, L. A.; Schiffmann, E.; Stracke, M. L. *Lipids Health Dis.* **2005**, *4*, 5.
41. Baker, D. L.; Fujiwara, Y.; Pigg, K. R.; Tsukahara, R.; Kobayashi, S.; Murofushi, H.; Uchiyama, A.; Murakami-Murofushi, K.; Koh, E.; Bandle, R. W.; Byun, H.-S.; Bittman, R.; Fan, D.; Murph, M.; Mills, G. B.; Tigyi, G. *J. Biol. Chem.* **2005**, *281*, 22786.
42. Cui, P.; Tonsig, J. L.; McCalmont, W. F.; Lee, S.; Becker, C. J.; Lynch, K. R.; Macdonald, T. L. *Bioorg. Med. Chem. Lett.* **2007**, *17*, 1634.
43. Durgam, G. G.; Virag, T.; Walker, M. D.; Tsukahara, R.; Yasuda, S.; Liliom, K.; van Meeteren, L. A.; Moolenaar, W. H.; Wilke, N.; Siess, W.; Tigyi, G.; Miller, D. D. *J. Med. Chem.* **2005**, *48*, 4919.
44. Gududuru, V.; Zeng, K.; Tsukahara, R.; Makarova, N.; Fujiwara, Y.; Pigg, K. R.; Baker, D. L.; Tigyi, G.; Miller, D. D. *Bioorg. Med. Chem. Lett.* **2006**, *16*, 451.
45. Jiang, G.; Xu, Y.; Fujiwara, Y.; Tsukahara, T.; Tsukahara, R.; Gajewiak, J.; Tigyi, G.; Prestwich, G. D. *ChemMedChem* **2007**, *2*, 679.
46. Ferry, G.; Moulharat, N.; Pradere, J. P.; Desos, P.; Try, A.; Genton, A.; Giganti, A.; Beucher-Gaudin, M.; Lonchampt, M.; Bertrand, M.; Saulnier-Blache, J. S.; Tucker, G. C.; Cordi, A.; Boutin, J. A. *J. Pharmacol. Exp. Ther.* **2008**, *327*, 809.
47. Prestwich, G. D.; Gajewiak, J.; Zhang, H.; Xu, X.; Yang, G.; Serban, M. *Biochim. Biophys. Acta* **2008**, *1781*, 588.
48. Zhang, H.; Xu, X.; Gajewiak, J.; Tsukahara, R.; Fujiwara, Y.; Liu, J.; Fells, J. I.; Perygin, D.; Parrill, A. L.; Tigyi, G.; Prestwich, G. D. *Cancer Res.* **2009**, *69*, 5441.
49. van Meeteren, L. A.; Ruurs, P.; Christodoulou, E.; Goding, J. W.; Takakusa, H.; Kikuchi, K.; Perrakis, A.; Nagano, T.; Moolenaar, W. H. *J. Biol. Chem.* **2005**, *280*, 21155.
50. Keller, T. H.; Pichota, A.; Yin, Z. *Curr. Opin. Chem. Biol.* **2006**, *10*, 357.
51. Lipinski, C. A.; Lombardo, F.; Dominy, B. W.; Feeney, P. J. *Adv. Drug Delivery Rev.* **2001**, *46*, 3.
52. Moulharat, N.; Fould, B.; Giganti, A.; Boutin, J. A.; Ferry, G. *Chem. Biol. Interact.* **2008**, *172*, 115.
53. Parrill, A. L.; Echols, U.; Nguyen, T.; Pham, T. C.; Hoeglund, A.; Baker, D. L. *Bioorg. Med. Chem.* **2008**, *16*, 1784.
54. Saunders, L. P.; Ouellette, A.; Bandle, R.; Chang, W. C.; Zhou, H.; Misra, R. N.; De La Cruz, E. M.; Braddock, D. T. *Mol. Cancer Ther.* **2008**, *7*, 3352.
55. Gijssbers, R.; Ceulemans, H.; Stalmans, W.; Bollen, M. J. *J. Biol. Chem.* **2001**, *276*, 1361.
56. Sakagami, H.; Aoki, J.; Natori, Y.; Nishikawa, K.; Kakehi, Y.; Natori, Y.; Arai, H. *J. Biol. Chem.* **2005**, *280*, 23084.
57. Stefan, C.; Jansen, S.; Bollen, M. *Trends Biochem. Sci.* **2005**, *30*, 542.
58. Tokumura, A.; Miyake, M.; Yoshimoto, O.; Shimizu, M.; Fukuzawa, K. *Lipids* **1998**, *33*, 1009.
59. Cui, P.; McCalmont, W. F.; Tonsig, J. L.; Lynch, K. R.; Macdonald, T. L. *Bioorg. Med. Chem.* **2008**, *16*, 2212.
60. Durgam, G. G.; Tsukahara, R.; Makarova, N.; Walker, M. D.; Fujiwara, Y.; Pigg, K. R.; Baker, D. L.; Sardar, V. M.; Parrill, A. L.; Tigyi, G.; Miller, D. D. *Bioorg. Med. Chem. Lett.* **2006**, *16*, 633.
61. van Meeteren, L. A.; Brinkmann, V.; Saulnier-Blache, J. S.; Lynch, K. R.; Moolenaar, W. H. *Cancer Lett.* **2008**, *266*, 203.
62. Koh, E.; Bandle, R. W.; Roberts, D. D.; Stracke, M. L.; Clair, T. *Lipids Health Dis.* **2009**, *8*, 4.
63. Lee, M. J.; Van Brocklyn, J. R.; Thangada, S.; Liu, C. H.; Hand, A. R.; Menzeleev, R.; Spiegel, S.; Hla, T. *Science* **1998**, *279*, 1552.
64. Ferguson, C. G.; Bigman, C. S.; Richardson, R. D.; van Meeteren, L. A.; Moolenaar, W. H.; Prestwich, G. D. *Org. Lett.* **2006**, *8*, 2023.
65. Zhou, M.; Diwu, Z.; Panchuk-Voloshina, N.; Haugland, R. P. *Anal. Biochem.* **1997**, *253*, 162.
66. Duan, R. D.; Bergman, T.; Xu, N.; Wu, J.; Cheng, Y.; Duan, J.; Nelander, S.; Palmberg, C.; Nilsson, A. *J. Biol. Chem.* **2003**, *278*, 38528.
67. Duan, R. D.; Cheng, Y.; Hansen, G.; Hertvig, E.; Liu, J. J.; Syk, I.; Sjostrom, H.; Nilsson, A. *J. Lipid Res.* **2003**, *44*, 1241.
68. Wu, J.; Nilsson, A.; Jonsson, B. A.; Stenstad, H.; Agace, W.; Cheng, Y.; Duan, R. D. *Biochem. J.* **2006**, *394*, 299.